DEVELOPMENT OF A NOVEL VORTEX FLOW METER FOR DOWNHOLE USE

Wouter Schiferli, Lun Cheng
TNO Science and Industry, Delft, The Netherlands

ABSTRACT

Due to the increasing complexity of oil and gas wells, the demand for instrumentation to measure conditions inside well tubing below the surface is growing rapidly. A robust meter was designed to measure fluid flows at downhole conditions. The meter is based on a specially-designed bluff body to detect vortex-induced pressure fluctuations and a fibre-optic Bragg grating sensor to transmit the vortex signal without the use of electronics downhole, a great advantage compared to many conventional flow meters.

The vortex flow meter was tested in water and oil, at pressures up to 6 bara, and was found to meet the requirements, functioning in a flow range of 0.3 – 7 m/s in a 3" pipe, at an accuracy better than ±6%.

1. INTRODUCTION

As easily accessible hydrocarbon reserves are decreasing, hydrocarbons must be produced from ever more complex reservoirs to meet demand. These reservoirs may consist of many sections separated by geological faults, or the oil may be very viscous, making production difficult. High oil prices have both increased the drive to produce additional hydrocarbons from a reservoir, and have made the use of complex technology to extract hydrocarbons economically viable.

The wells drilled in many reservoirs have become increasingly complex. In fractured reservoirs, hydrocarbons may be produced from many different zones separated by geological fractures, often requiring multilateral (branched) wells.

Hydrocarbon production leads to a decreasing reservoir pressure, which eventually makes it impossible to produce a reservoir naturally, since reservoir pressure is no longer sufficient to drive the hydrocarbons towards the surface. This marks the end of primary production.

Secondary production allows production to continue. This involves drilling extra injector wells to inject water or gas into the reservoir. This restores reservoir pressure and displaces hydrocarbons from the reservoir rock. In order to maximize yield from the reservoir, it is important to choose injection sites carefully. With multiple injection or production points, it becomes important to measure the flow distribution between the various points, to optimize reservoir production. In order to achieve this, it would be advantageous to install flow meters at various intervals in injection wells, measuring the amount of fluid injected at a each location.

This need formed the background of this development. Current flow meters suited to the operating conditions at the bottom of injection wells are expensive, making the deployment of multiple meters in a single injection well very costly. A robust, simple meter was developed to meet the need for downhole instrumentation.

2. METER REQUIREMENTS

The current vortex flow meter is developed for use in water injection wells, but with additional engineering, it can be made available for gas and high temperature steam applications too. Generally, the downhole conditions are harsh and impose specific requirements on the vortex flow meter. For example, it must be robust and able to withstand temperatures up to 350°C when used in steam applications and pressures up to 400 bar.

Better than 10% accuracy was desired, in a flow range of 0.5 to 5 m/s for water in a 3" tubing. For the intended application in injection wells, very high absolute accuracy is not required.

Downhole instrumentation is packaged in a section of tubing, which is inserted as part of a complete well string, a full set of tubing forming the well itself. The meter may be located several kilometers under the surface, making access only possible by taking all the well tubing to the surface, until the meter reaches the surface. This makes servicing the meter a very expensive operation. This underlines the need for a robust flow meter.

Under these conditions, the use of electronics is undesirable. An optical fibre incorporating a Bragg grating was used to meet this condition, providing a method to detect strain caused by vortex shedding without the use of piezo-electric sensors, as well as transmitting the signal optically rather than electronically, eliminating the need for signal amplifiers.

The use of a Bragg grating imposes specific requirements on the meter. The bluff body has to be designed such that the pressure fluctuations produced by vortex shedding may be detected as mechanical strain by the Bragg grating.

Maximum pressure	400 bar
Maximum temperature	350 °C
Lower flow limit	0.5 m/s water
Upper flow limit	5 m/s water
Accuracy	better than 10%
Inner diameter	3" (80 mm)

Table 1: Summary of requirements

3. METER DESIGN

3.1 Bluff body design

The role of the bluff body in a vortex flow meter is to produce well-defined vortices. In order to measure flow, the frequency of these oscillations must be measured. When using a fibre Bragg grating, the measured quantity is strain, not pressure. The bluff body must therefore contain a section where the pressure fluctuations translate into a level of strain that is measurable by an FBG.

3.1.1 Vortex shedding optimization

A vortex flow meter is based on the principle of vortex shedding on an obstacle (bluff body) placed in the flowing fluid. A boundary layer grows on both sides of the bluff body because of viscosity and separates. The vortices separate alternately on both sides of the body. The vortex shedding frequency f is proportional to the flow velocity U, according to:

$$f = St\frac{U_0}{W} \qquad (1)$$

St is the Strouhal number, a dimensionless constant and W the width of the bluff body. The Strouhal number is characteristic for a certain bluff body shape and is constant in a certain range of the Reynolds number. Although the shedding frequency naturally varies in time, some design criteria have to be considered to minimize these variations to typically 10 - 20%:

- conditioning the flow past the bluff body;
- introducing end-plates on the bluff body;
- introducing boundary layer control techniques on the bluff body.

The flow can be conditioned by placing the bluff body many diameters downstream from bends and other obstacles. The pipe wall can act as end-plates and the boundary layer can be controlled by having well-defined separation points on the bluff body (sharp edges).

These sharp edges are also important to have a constant Strouhal number as function of the Reynolds number for the bluff body. Signal processing can improve results by using, for example, long sampling times averaging out frequency fluctuations.

Another important factor is the pressure drop over the flow meter. The pressure drop is a quadratic function of the flow velocity and linear to the inverse of the bluff body width. In literature often a quarter of the pipe diameter for the bluff body width is mentioned as optimum between pressure drop and regular vortex shedding (Baker, 2000).

Literature (El Wahed et al., 1991) indicates a T-shaped shedder gives the best signal quality. The characteristics of a T-shaped shedder are further explored by Miau et al. (1993), who give the ideal range of the tail length with respect to bluff body size. They indicate an L/W ratio of 1.56 – 2.0 gives the clearest signal, in which low-frequency fluctuations are suppressed, and the signal is dominated by the vortex-induced frequency peak.

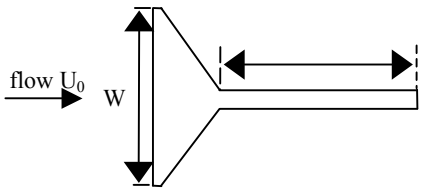

Figure 1: *Bluff body geometry*

Basic body geometry is given in Table 2:

Body width W	20 mm
Tail length L	36 mm
Tail width D_{tail}	next section

Table 2: Bluff body dimensions

Note that the tail length used corresponds to an L/W ratio of 1.8. An added advantage of using a T-shaped body to generate vortices is that the FBG sensor can be integrated into the tail, which is relatively thin, and where the vortex shedding can generate sufficient strain.

The maximum frequency of the vortex shedding can be deduced from equation (1) if the geometry's characteristic Strouhal number is known. This was obtained using a Discrete Vortex Method (DVM) based code. In such methods, which are grid free and generally computationally less intensive than conventional CFD, the body surface is divided into panels, from which discrete vortices are released. This introduces vorticity into an otherwise potential flow.

At several points in the wake, marked by blue crosses, pressure and flow were calculated. *Figure 2* shows results from the calculations, with each dot indicating a discrete vortex.

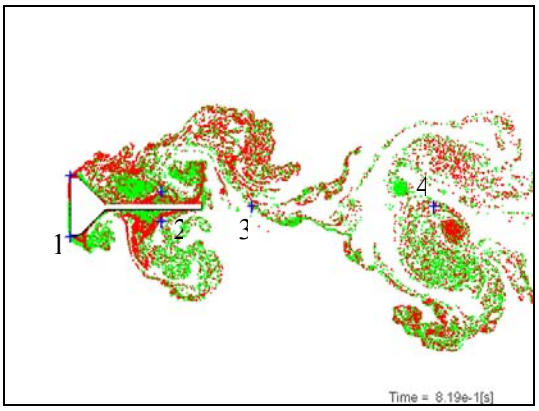

Figure 2: *Results obtained using DVM*

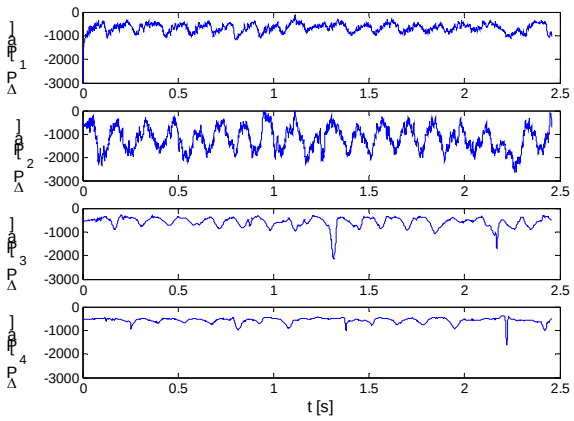

Figure 3: *Pressure fluctuations*

Figure 3 shows that predicted pressure fluctuations are largest at position 2. A Fourier transform of these signals yields a peak at around 7 Hz for 1 m/s flow velocity, corresponding to Sr = 0.14 – 0.15, depending on the position.

The expected frequency of the pulsations in the actual prototype can now be calculated:

Velocity [m/s]	f [Hz]
0.5	3.75
5.0	37.5

Table 3: Expected frequencies

This frequency range forms a requirement for the FBG sensor.

3.1.2 Integrating the FBG sensor

A FBG sensor consists of an optical fibre in which a grating has been etched. This grating reflects light at a well-defined wavelength, determined by the grating spacing. Stretching the fibre will change the grating spacing, and therefore frequency. Specifications of the read-out unit used are:

Min. measurable strain	1 µm/m
Max. sampling frequency	1000 Hz

Table 4:FBG sensor specifications

Note from Table 3 that the frequency of fluctuations lies well within the measurable frequency range.

The pressure fluctuation due to vortex shedding cause an alternating bending of the plate. The resulting strain is maximum where the tail is attached to the thicker bluff body, as Figure 4 shows. This is the optimum location for the FBG.

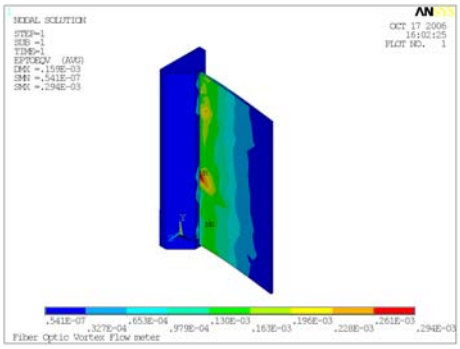

Figure 4: *Calculated strain*

The thickness of the plate determines the deflection, and ultimately meter sensitivity. The strain in the plate in response to a pressure fluctuation was calculated in an ANSYS mechanics FEM calculation. A tail thickness of 1 mm was calculated to give sufficient sensitivity at 0.5 m/s.

3.1.3 Final prototype

Based on these calculations, a prototype flow meter was produced. The fibre containing the Bragg grating was embedded in the groove in the tail. Both tail length and thickness can be varied to evaluate the effect on signal quality by changing the tail section.

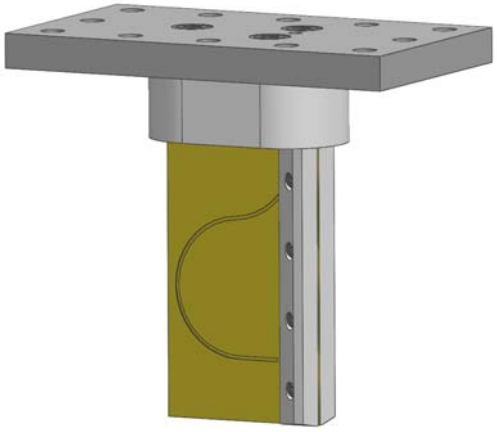

Figure 5: *Prototype, showing location of the fibre groove*

4. EXPERIMENTAL RESULTS

Several sets of experiments were performed. Initial tests were conducted on an in-house water rig, at unpressurized conditions, at velocities between 0.2 and 7 m/s. At the upper boundary of this flow range cavitations occurred.

The measurements shown below were performed for periods of 30s. An FFT was taken over this full time period to find the frequency of pressure pulsations.

4.1 Operation in water

To function as a flow meter, the relationship between flow rate and frequency should be consistent and ideally linear. Figure 6 confirms this linear relationship, which was obtained by stepping up the flow to the maximum flow, and decreasing it in discrete steps to low values.

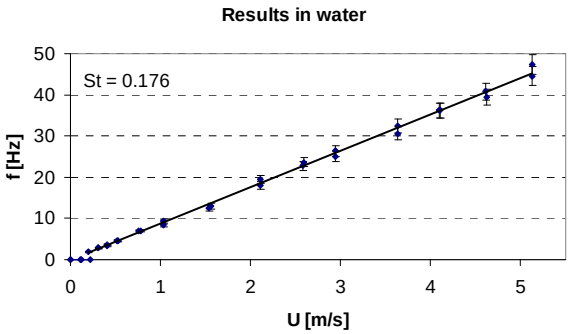

Figure 6: *Results obtained in water*

The minimum velocity at which a clear frequency peak was still present is 0.3 m/s. Since the required minimum is 0.5 m/s, the meter meets requirements. Error bars correspond to ±5% error. For the above test, all data points lie within this error range from a linear trend. In general, 96% of the points fell within an error band of ±6%.

Note that the Strouhal number is slightly higher than predicted by initial calculations. This may be due to blockage effects, which slightly raise local velocities, and were not taken into account when performing the calculations.

The peak in the frequency spectrum is well-defined, as Figure 7 shows. This signal was taken at 2.75 m/s flow velocity, corresponding to a 22 Hz vortex frequency.

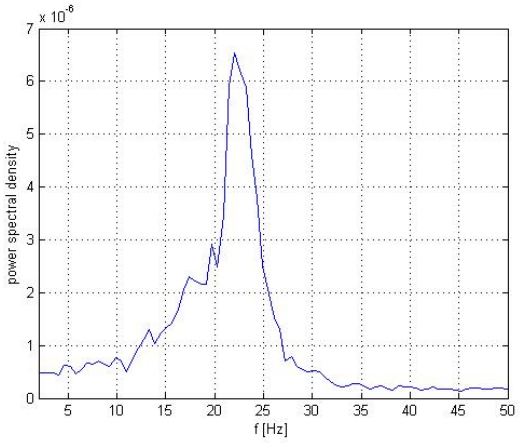

Figure 7: *Power spectrum at 2.75 m/s*

Table below gives Reynolds number at various flow rates, in water. The first Reynolds number is stated with respect to the tubing diameter D of 0.082 m, showing that all flows are turbulent. The second Reynolds number, Re_W is calculated relative to bluff body width W. This Reynolds number determines the nature of the vortex shedding.

U_0 [m/s]	Re	Re_W
0.25	2.0×10^4	5.0×10^3
0.50	4.0×10^4	1.0×10^4
5.00	4.0×10^5	1.0×10^5

Table 5: Reynolds number range in water

Note in Figure 6 that it proved possible to distinguish a frequency peak at velocities as low as 0.2 m/s. Detection of the peak is limited by the fact that low-frequency noise is present in the signal. At 0.2 m/s, frequencies lie around 1.7 Hz, which is difficult to filter from low-frequency noise.

Vortex shedding is coherent down to at least a Re_W of 5000. Below this value the vortex signal could no longer be discriminated from low-frequency fluctuations present in the strain measurements.

4.2 Effect of pressure

At different pressures, the meter functions identically. Note that this has negligible effect on density since the fluid is water. An effect of pressure would therefore not have been expected.

Since the fluid is water, which may be considered incompressible, Re is not affected by the higher pressure. Vortex shedding would therefore not be expected to change.

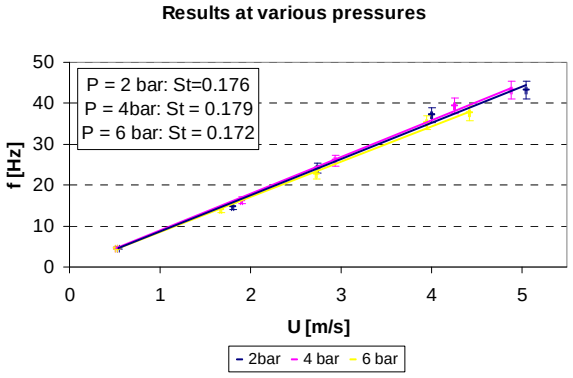

Figure 8: *Operation in water at various pressures*

4.3 Operation in oil

Again, the flow meter functions as expected, at identical Sr.

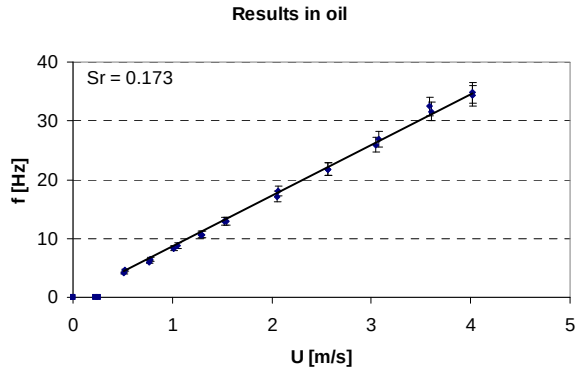

Figure 9: *Operation in oil*

At operating conditions of 40°C, oil density is 849 kg/m^3, and oil viscosity is 10 mm^2/s, or a kinematic viscosity of 8.5×10^{-3} Pa s.

U_0 [m/s]	Re	Re_W
0.50	4×10^3	1×10^3
5.00	4×10^4	1×10^4

Table 6: Reynolds number range in oil

Vortex shedding is still coherent at Re_D = 1000, where the flow meter still shows linear behaviour and vortex shedding occurs at approximately 4 Hz. At lower velocities, no clear frequency peak is observed, despite the fact that the amplitude of fluctuations is similar to that in water at higher velocities. At these low Reynolds numbers below 1000, vortex shedding appears to break down.

5. CONCLUSION

A prototype fibre-optic vortex meter was constructed and tested in water and oil. The measurement principle relies on fluid-structure interaction between the vortex street in the wake of the meter, and a tail section added to a triangular bluff body. The specific shape, therefore, allows the bluff body to combine two functions: a stiff bluff body to generate vortices, and a more flexible section with integrated fibre Bragg grating, designed to measure the generated pressure fluctuations.

In order to be able to measure flow, the mechanical strain has to be of sufficient magnitude to be detected by the FBG sensor. This was ensured by coupling a calculation of expected pressure fluctuations to a finite elements mechanics calculation.

The prototype meter met all requirements for accuracy and turn-down ratio in water and oil flows, proving that the measurement principle is sound. Some further optimization is desired to maximize signal quality. Once further optimization has been performed, the resulting optimum design must be made into a rugged prototype for testing. A project to achieve these goals is ongoing.

6. REFERENCES

El Wahed, A.K., Sproston, J.L., 1991, The influence of shedder shape on the performance of the electrostatic vortex flowmeter. *Flow Measurement Instrumentation,* **Vol 2**: 169-179

Miau, J.J., Yang, C.C., Chou, J.H., Lee, K.R., 1993, A T-shaped vortex shedder for a vortex flowmeter. *Flow Measurement Instrumentation,* **Vol 4 No 4**: 259-267

Baker, R.C., 2000, *Flow measurement handbook*, Cambridge University Press.

ACKNOWLEDGEMENT

The authors would like to thank Shell International Exploration and Production (SIEP) for their technical input and financial support, and for using their world-class multiphase flow loop at Shell EPiCentre, Rijswijk, The Netherlands, .